The Plant Cell, Vol. 23: 2553–2567, July 2011, www.plantcell.org 

# *Arabidopsis* Class I KNOTTED-Like Homeobox Proteins Act Downstream in the IDA-HAE/HSL2 Floral Abscission Signaling Pathway [C][W][OA]

**Chun-Lin Shi,[a] Grethe-Elisabeth Stenvik,[a,1,2] Ane Kjersti Vie,[b,1] Atle M. Bones,[b] Véronique Pautot,[c] Marcel Proveniers,[d] Reidunn B. Aalen,[a] and Melinka A. Butenko[a,3]**

[a] Department of Molecular Biosciences, University of Oslo, N-0316 Oslo, Norway
[b] Department of Biology, Norwegian University of Science and Technology, N-7491 Trondheim, Norway
[c] Institut Jean-Pierre Bourgin, Unité Mixte de Recherche 1318 Institut National de la Recherche Agronomique-Agro Paris Tech, Bâtiment 2, Institut National de la Recherche Agronomique Centre de Versailles-Grignon, 78026 Versailles Cedex, France
[d] Molecular Plant Physiology, Department of Biology, Faculty of Science, Utrecht University, 3584 CH Utrecht, The Netherlands

**Floral organ abscission in *Arabidopsis thaliana* is regulated by the putative ligand-receptor system comprising the signaling peptide INFLORESCENCE DEFICIENT IN ABSCISSION (IDA) and the two receptor-like kinases HAESA and HAESA-LIKE2. The IDA signaling pathway presumably activates a MITOGEN-ACTIVATED PROTEIN KINASE (MAPK) cascade to induce separation between abscission zone (AZ) cells. Misexpression of IDA effectuates precocious floral abscission and ectopic cell separation in latent AZ cell regions, which suggests that negative regulators are in place to prevent unrestricted and untimely AZ cell separation. Through a screen for mutations that restore floral organ abscission in *ida* mutants, we identified three new mutant alleles of the *KNOTTED-LIKE HOMEOBOX* gene *BREVIPEDICELLUS* (*BP*)/*KNOTTED-LIKE FROM ARABIDOPSIS THALIANA1* (*KNAT1*). Here, we show that *bp* mutants, in addition to shedding their floral organs prematurely, have phenotypic commonalities with plants misexpressing *IDA*, such as enlarged AZ cells. We propose that *BP*/*KNAT1* inhibits floral organ cell separation by restricting AZ cell size and number and put forward a model whereby IDA signaling suppresses BP/KNAT1, which in turn allows *KNAT2* and *KNAT6* to induce floral organ abscission.**

## INTRODUCTION

Cell separation processes are critical for the development of a plant and play key roles from sculpting the form of the plant to scattering seeds. Abscission, a physiological process that involves programmed changes in cellular adhesion, allows the plant to discard nonfunctional or infected organs. At the cellular level, the presence of an abscission zone (AZ), consisting of small densely cytoplasmic cells at the boundary between organ and plant, is a prerequisite for abscission to take place (McKim et al., 2008). During the subsequent activation of the cell separation process, AZ cells acquire competence to respond to abscission signals and secrete cell wall–modifying and hydrolyzing enzymes that act to degrade the middle lamella between two adjacent cell files (Bleecker and Patterson, 1997; Patterson, 2001; Roberts et al., 2002; Lewis et al., 2006; Stenvik et al., 2006). Shortly before organ shedding, the cells at the proximal side of the AZ expand; however, the relationship between AZ cell enlargement and organ separation is unclear (Patterson, 2001). It has been proposed that the functional role of AZ cell expansion might be to create the tension needed for the final mechanical rupture of the AZ (Sexton and Redshaw, 1981); indeed, the receptor-like kinase (RLK) *EVERSHED* (*EVR*) has recently been implicated in regulating the proper timing of floral organ abscission in *Arabidopsis thaliana* in part by restricting AZ cell size (Leslie et al., 2010).

The correct temporal and spatial regulation of abscission is crucial during plant development. Premature abscission of reproductive organs or immature seeds can compromise reproduction, and unrestricted cell separation can lead to shedding of organs in the proximity of activated AZ cells or interfere with tissue integrity. Studies using *Arabidopsis* have implicated the involvement of several different genes in the control of floral organ abscission (Aalen, 2011), including a newly identified putative peptide ligand-receptor system (Cho et al., 2008; Stenvik et al., 2008).

Recently, it was discovered that HAESA (HAE) and HAESA-LIKE2 (HSL2), a pair of leucine-rich repeat (LRR)-RLKs, are redundantly required for regulating cell separation during floral organ abscission in *Arabidopsis* (Cho et al., 2008; Stenvik et al., 2008). *hae hsl2* double mutants are phenotypically similar to plants with mutations in *INFLORESENCE DEFICIENT IN ABSCISSION* (*IDA*) (Cho et al., 2008; Stenvik et al., 2008). *IDA*

[1] These authors contributed equally to this work.
[2] Current address: Section of Cancer Cytogenetics, Institute for Medical Informatics, Oslo University Hospital, 0424 Oslo, Norway.
[3] Address correspondence to m.a.butenko@imbv.uio.no.
The author responsible for distribution of materials integral to the findings presented in this article in accordance with the policy described in the Instructions for Authors (www.plantcell.org) is: Melinka A. Butenko (m.a.butenko@imbv.uio.no).
[C] Some figures in this article are displayed in color online but in black and white in the print edition.
[W] Online version contains Web-only data.
[OA] Open Access articles can be viewed online without a subscription.
www.plantcell.org/cgi/doi/10.1105/tpc.111.084608

encodes a protein with features compatible with it being a peptide ligand (Stenvik et al., 2008) and is essential for the final separation step of floral abscission (Butenko et al., 2003). *ida* mutant plants are completely deficient in floral organ abscission, and overexpression of the IDA protein leads to premature abscission, an excessively enlarged floral AZ region and ectopic cell separation in vestigial AZs of organs that normally do not abscise in *Arabidopsis* (Stenvik et al., 2006). In addition, these plants secrete a white substance at organ detachment points consisting mainly of arabinogalactan (AG) (Stenvik et al., 2006). Genetic interaction studies demonstrated that functional receptors are essential for IDA to exert its function (Cho et al., 2008; Stenvik et al., 2008). In addition, genetic studies and in vitro kinase assays showed that the MITOGEN-ACTIVATED PROTEIN KINASE KINASE4 (MKK4) and MKK5 and MAPK3 and MAPK6 act downstream of IDA, HAE, and HSL2 (Cho et al., 2008). Consequently, there seems to be a core signaling pathway regulating cell separation in floral abscission.

A number of mutants have been identified that impediment abscission; the double mutant of the *BLADE-ON-PETIOLE1* (*BOP1*) and *BOP2* genes does not differentiate anatomically distinct AZ cells and is consequently completely deficient in abscission (Hepworth et al., 2005; Norberg et al., 2005; McKim et al., 2008). In addition, the recently described mutant *nevershed* (*nev*) with a mutation in a gene encoding an ADP-ribosylation factor-GTPase-activating protein (Liljegren et al., 2009) has a complete lack of floral abscission. *NEV* has been implicated in regulating the proper timing of abscission by trafficking key factors required for cell separation and/or for the trafficking of receptor complexes (Liljegren et al., 2009). Interestingly, a suppression screen on *nev* identified mutations in the LRR-RLKs *EVR* and *SOMATIC EMBRYOGENESIS RECEPTOR KINASE1* (*SERK1*), which in combination with *nev* showed precocious floral abscission and enlarged AZ regions reminiscent of those seen in plants overexpressing IDA (Leslie et al., 2010; Lewis et al., 2010). The mechanisms that prevent premature organ separation are largely unknown, but EVR and SERK1 may function as inhibitors of this step in the abscission process. However, both *evr* and *serk1* single mutants have seemingly normal abscission and neither could rescue the abscission defect of *ida* or *hae hsl2*, indicating that other factors must be acting as repressors downstream in the IDA-HAE/HSL2 pathway.

To identify additional components of the IDA signaling pathway, we screened progeny of mutagenized *ida-1* seeds (Butenko et al., 2003) for normal floral organ abscission. Here, we report the identification and analysis of new alleles of the *KNOTTED*-like homeobox gene (*KNOX*), *BREVIPEDICELLUS* (*BP*)/*KNOTTED-LIKE FROM ARABIDOPSIS THALIANA1* (*KNAT1*), which suppresses the *ida* mutation. The *bp* mutants exhibit similar phenotypes to those observed in plants overexpressing IDA and were also capable of rescuing the abscission defect of *hae hsl2*. We therefore propose that *BP*/*KNAT1* is important in regulating the correct timing of organ separation by restricting AZ cell size and is a component in the IDA-HAE/HSL2 signaling pathway. We show that two closely related genes in the class I KNOX subfamily, *KNAT2* and *KNAT6* (Scofield and Murray, 2006; Mukherjee et al., 2009), are likely to act as activators of floral organ separation in close connection with *BP*/*KNAT1*. The role of *KNAT2* and *KNAT6* in the floral abscission process and their genetic relationship to *IDA* is discussed.

## RESULTS

### A Suppressor Screen to Identify Components of the IDA Signaling Pathway

Wild-type floral organs abscise shortly after anthesis (Figures 1A and 1B), whereas the perianth and stamens remain attached indefinitely in null alleles of *ida* (Figures 1C to 1F). We reasoned that it should be possible to identify essential components of the IDA signaling pathway in a screen for suppressor mutants (Figure 1G). After ethyl methanesulfonate mutagenesis, M2 plants generated from mutagenized *ida-1* seeds (Butenko et al., 2003) (Figures 1C and 1D) were screened for their ability to undergo floral abscission. Progeny from 13,000 M1 plants were analyzed, and 16 mutant lines were recovered. Three lines partially rescued the abscission defect of *ida-1*, whereas the remaining thirteen lines showed normal floral abscission. Two of the mutant lines (lines 49 and 595) identified had, in addition to normal organ shedding, the characteristic downward-pointing silique phenotype conferred by mutations in the *KNOX* gene *BP*/*KNAT1* (Douglas et al., 2002; Venglat et al., 2002) (Figures 1H and 1J; see Supplemental Figure 1A online). An additional mutant line (line 221) portrayed a partial rescue of the *ida-1* abscission defect and a less severe bending of the siliques (see Supplemental Figures 1B and 1C online). Crosses between the three mutant lines verified that they were in the same complementation group. Because the phenotypes of lines 49 and 595 were indistinguishable, analysis was performed using line 49.

The F2 progeny of line 49 crossed to C24 wild type segregated for wild type or *ida* phenotype and plants with a *bp*-like silique phenotype in a 3:1 ratio ($n = 48$, segregating 37:11), showing that the mutation in line 49 is fully recessive. Two of the 11 plants with the *bp*-like silique phenotype were wild-type for the *IDA* alleles (Figure 1L), whereas four were homozygous for the T-DNA insertion of *ida-1*, confirming that the mutation in line 49 was responsible for the revertant floral phenotype observed.

Mutations in *IDA* block abscission at the stage when the AZ cells undergo separation; the early steps in the floral abscission process from AZ cell patterning and differentiation to initial organ loosening remain mainly unaffected (Butenko et al., 2003; Stenvik et al., 2006). A stress transducer was used to quantify the force needed to remove petals from the receptacle of the plant, the petal breakstrength (pBS), during the abscission process (Fernandez et al., 2000; Lease et al., 2006). Similar to the wild type, the *ida-1* mutant has a high pBS, exceeding 2 g equivalents at positions 2 and 4 (referring to location when counting flowers from anthesis along the inflorescence, according to Bleecker and Patterson [1997]) (Figure 1N). *ida-1* shows a gradual decrease in pBS from position 4 to 10, which is indicative of initial cell wall loosening, but the decline is delayed by two positions compared with wild-type flowers (Figure 1N) (Butenko et al., 2003). For *ida-1*, but not the wild type, there is a gradual increase in pBS from position 10, and flowers at position 20 have pBS similar to those at position 6 (Figure 1N). Line 49 had a pBS profile

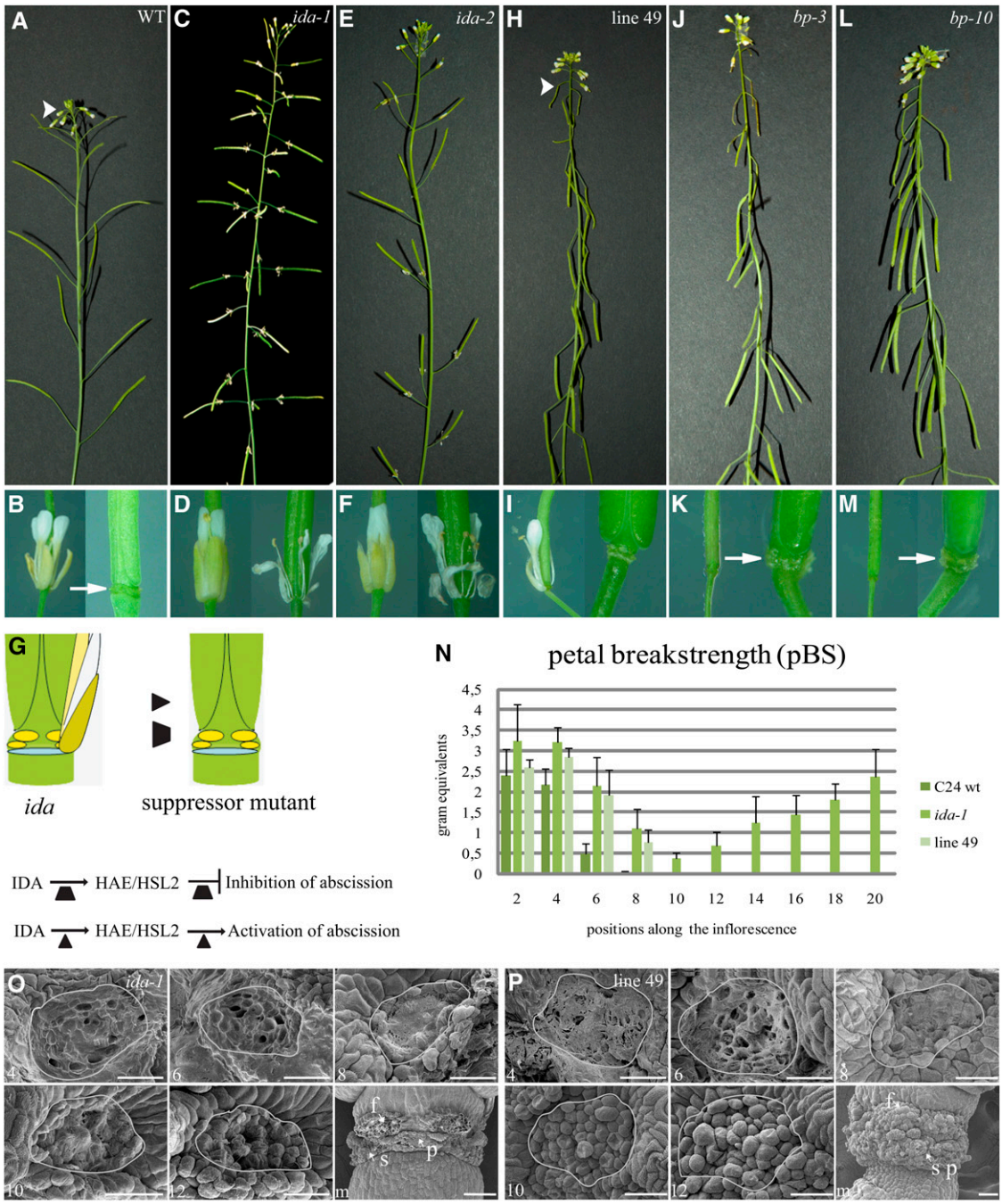


**Figure 1.** Phenotypes of *ida* and *bp* Mutants.

**(A)** and **(B)** C24 wild-type (WT) plants undergo flower abscission shortly after anthesis, which defines position 1 when counting flowers along the primary inflorescence (arrowhead). At position 7 (left image in **[B]**) turgid petals and senescent sepals are still attached to the receptacle of the flower. The AZ region at position 12 (arrow) after floral organs have abscised is shown on the right in **(B)**.

**(C)** to **(F)** *ida-1* (C24; **[C]** and **[D]**) and *ida-2* (Col; **[E]** and **[F]**) retain floral organs indefinitely. Position 7 (left in **[D]** and **[F]**) and position 12 (right in **[D]** and **[F]**).

**(G)** Cartoon illustrating suppression screen of *ida-1*. Revertant mutants portraying normal abscission could either be mutated downstream inhibitors (blunt arrowheads) in the IDA signaling pathway or constitutively active components (arrowheads) of the pathway.

**(H)** and **(I)** Line 49 with downward-pointing siliques and abscised floral organs by position 9 (arrowhead). AZ with floral organs attached at position 7 (left in **[I]**) and abscised at position 12 (right in **[I]**).

**(J)** and **(K)** *bp-3* mutant with downward-pointing siliques and abscised floral organs by position 7 (left in **[K]**) and an enlarged AZ region at position

similar to that of *ida-1* until position 8 (Figure 1N); however, there was no increase in the pBS past position 8, and by position 9, all floral organs had abscised from line 49 (Figure 1I).

pBS measurements are supported by anatomical observations in scanning electron micrographs of AZ cells during the course of floral abscission. pBS values above 2 are associated with the presence of broken cells at the fracture plane between the petal and the body of the plant due to high forces keeping the cell walls together. This corresponds to flowers up to position 4, capable of responding to abscission signals such as ethylene (Butenko et al., 2003) but which still have their cell walls intact. pBS values under 1.5, observed from position 6, reveal a flattened fracture cavity, indicating an initial degradation of the middle lamella between two adjacent AZ cells and an initial cell wall loosening. Measurements below 0.5 are linked to initial rounding of cells and are observed shortly before the actual separation step (Patterson and Bleecker, 2004). When AZ cells are fully expanded, the organ abscises and the pBS is no longer assessable. pBS can therefore be used to characterize the changes AZ cells undergo during abscission, and it is a powerful tool for analyzing where in the abscission process a mutant is affected.

We compared the fracture surface of the petal AZ of *ida-1* to that of line 49 by either forceful removal of the petal or natural shedding at different stages of development (Figures 1O and 1P). The exposed cell surface of both mutant lines looked similar up to position 8; however, at position 10, the stage of organ separation for C24 wild-type flowers, line 49 had fully rounded cells, whereas *ida-1* still displayed a flattened cavity (Figures 1O and 1P). At position 12, the petal AZ cells of line 49 had expanded further, whereas those of *ida-1* had not. Interestingly, the AZs of mature siliques in line 49 were enlarged compared with the wild type (see Figure 3C), making it impossible to discern between petal and sepal AZ as these were merged together (Figure 1P), a phenotype similar to that observed in plants overexpressing *IDA* (Stenvik et al., 2006). In AZs of mature *ida-1* siliques, broken cells were observed due to incomplete dissolution of the middle lamella and failure to undergo organ separation (Figure 1O). The reversion of pBS to wild-type levels and the full rounding of AZ cells in line 49 led us to conclude that the affected gene in this mutant was involved in regulating the separation event of floral organ abscission, conceivably as a component of the *IDA* signaling pathway.

As a result of the similar silique phenotype between line 49 and the *bp* mutant, we sequenced the *BP*/*KNAT1* gene in line 49 and identified a nucleotide difference in the second exon, causing a premature stop codon in the KNOX2 domain (see Supplemental Figures 1D and 1E online). Two different mutation sites in *BP*/*KNAT1* were found for lines 595 and 221, causing a change in the splice acceptor site of intron one and an amino acid exchange in the homeodomain (HD), respectively (see Supplemental Figures 1D and 1E online). A 3267-bp genomic fragment containing the coding sequence of *BP*/*KNAT1* under the control of the cauliflower mosaic virus *35S* promoter was sufficient to complement the downward-pointing siliques of line 49, and the plants showed the characteristic *35S*:*KNAT1* phenotypes, such as lobed leaves and floral organ defects (Lincoln et al., 1994; Chuck et al., 1996) (see Supplemental Figure 1F online). Therefore, we concluded that the mutations singled out in the *BP*/*KNAT1* gene in lines 49, 595, and 221 restored full or partial cell separation within *ida-1* AZs.

To substantiate the ability of a mutation in *BP*/*KNAT1* to rescue the abscission phenotype of *ida*, a Columbia (Col) null-allele deletion mutant of *BP*/*KNAT1*, *bp-3* (Rim et al., 2009) (see Supplemental Figure 1G online), was crossed to *ida-1* and *ida-2* and both double mutants portrayed wild-type floral abscission (see Supplemental Figures 2A to 2C online). The observed phenotypes were substantiated by pBS (see Supplemental Figure 2F online), and mature AZs of the double mutants were covered with a white substance similar to that covering AZs of plants overexpressing *IDA* (see Supplemental Figures 2D and 2E online).

Given the confirmation of the molecular nature of line 49, it will from now on be referred to as *bp ida-1* and the single mutant obtained from backcross to C24 as *bp-10*.

### *BP*/*KNAT1* Prevents Premature Floral Organ Abscission

The rescue of organ separation in *bp ida-1*, *bp-3 ida-1*, and *bp-3 ida-2* flowers suggests an important role for *BP*/*KNAT1* in the developmental control of floral organ abscission. Therefore, we first determined whether *BP*/*KNAT1* was expressed in a temporal and spatial manner compatible with modulating floral abscission using a *promoter*:*GUS* (for β-glucuronidase) transgene (*BP*/*KNAT1*$_{pro}$:*GUS*) according to Ori et al. (2000). GUS expression was first detected in the pedicels of the inflorescence apex and the replum of the gynoecium (see Supplemental Figure 3A online) as shown by Douglas et al. (2002), Alonso-Cantabrana et al. (2007), and Ragni et al. (2008). From flower position one, also defined as stage 13 by Smyth et al. (1990), there was weak GUS staining in the AZ and at the base of the pedicel (see Supplemental Figures 3B and 3C online). This low level of expression was maintained until position 4, from which point there was a strengthened GUS signal that reached a peak at position 8-10, corresponding to the phase at which organs detach, and was

**Figure 1.** (continued).

12 (arrow, right in **[K]**)

**(L)** and **(M)** Segregants from line 49 backcrossed to the C24 wild type with downward-pointing siliques and abscised floral organs by position 7 (left in **[M]**) and an enlarged AZ region at position 12 (arrow, right in **[M]**).

**(N)** pBS (i.e., the force required to remove the petals from the flower) of line 49 compared with *ida-1* and C24 wild-type (wt) flowers ($n$ = 15, bars = SD).

**(O)** and **(P)** Scanning electron micrographs of fracture planes of petal AZ (delineated in gray) and the entire AZ region of mature siliques of *ida-1* **(O)** and line 49 **(P)**. Arabic numerals indicate floral positions along the inflorescence. m, mature siliques; f, filament AZ; p, petal AZ; s, sepal AZ. Note that for mature siliques of line 49, it is not possible to distinguish the petal and sepal AZs from each other.

Bars = 30 μm for positions 4 to 12 and 100 μm in mature siliques.

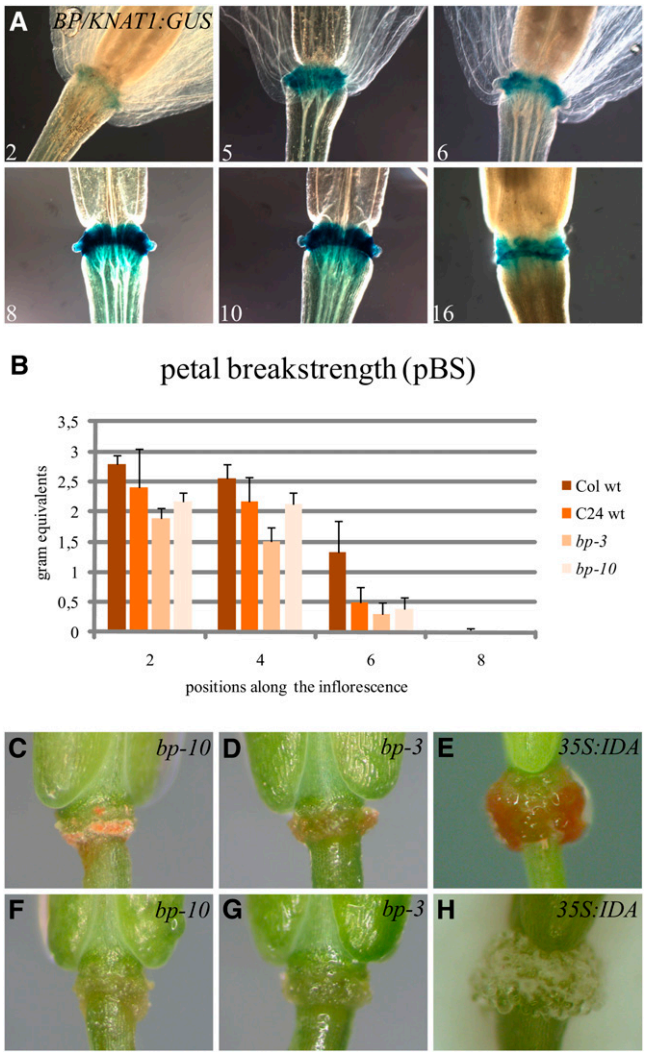


**Figure 2.** *BP/KNAT1* Involvement in Floral Abscission.

**(A)** *BP/KNAT1*$_{pro}$*:GUS* expression during floral organ abscission. Arabic numerals indicate floral positions along the inflorescence.
**(B)** pBS of *bp-3* and *bp-10* mutants compared with Col wild-type (wt) and C24 wild-type flowers, respectively ($n$ = 15, bars = SD).
**(C)** to **(E)** Mature siliques stained with the Yariv reagent β-GLcY, resulting in a red precipitate.
**(F)** to **(H)** Mature siliques stained with the negative control α-GLcY.

then gradually diminished (Figure 2A). A GUS signal could be detected in the AZ as late as position 16, showing that *BP/KNAT1* expression was maintained after the floral organs had abscised, indicating that *BP/KNAT1* could also play a role after floral organ shedding. The initial augmentation in *BP/KNAT1* expression at position 5-6 (Figure 2A) corresponded to the stage at which the pBS was markedly reduced in wild-type petals prior to organ shedding (Figure 1N) and coincides with the onset of *IDA*$_{pro}$*:GUS* expression (Butenko et al., 2003). Moreover, the *BP/KNAT1*$_{pro}$*:GUS* profile was similar to the reported expression patterns of *HAE*$_{pro}$*:GUS* and *HSL2*$_{pro}$*:GUS* (Jinn et al., 2000; Cho et al., 2008; Leslie et al., 2010). This expression pattern suggests that *BP/KNAT1* can have a role in both the initial stages of floral abscission, prior to organ dissociation, as well as regulating cell separation.

It has been suggested that *BP/KNAT1* could be involved in regulating AZ cell formation (Wang et al., 2006). Loss-of-function *bop1 bop2* double mutants lack floral organ abscission due to an inability to specify the anatomy of AZ cells (McKim et al., 2008) (see Supplemental Figure 3D online). We created *bop1 bop2 bp-3* and *bop1 bop2 bp ida-1* to investigate whether the absence of *BP/KNAT1* would have an effect on the abscission phenotype of *bop1 bop2* plants. Floral organ abscission was not reestablished in *bop1 bop2 bp-3* and *bop1 bop2 bp ida-1* plants (see Supplemental Figures 3E and 3F online). Thus, mutations in *BP/KNAT1* are not sufficient to initiate AZ formation, suggesting that the reported enlargement of floral AZs (Wang et al., 2006) is dependent on the presence of morphologically distinct AZ cells.

Differences in pBS profiles between mutant and wild-type plants provide information as to where in the abscission process the mutation is exerting its effect (Patterson and Bleecker, 2004). The pBS of *bp-3* and *bp-10* was compared with that of Col wild-type and C24 wild-type plants, respectively. For *bp-3*, but not *bp-10*, there was a substantial reduction in pBS at all measurable positions (Figure 2B), indicating that *bp-3* has a precocious dissolution of the middle lamella between petal AZ cells. The floral organs of *bp-3* were also shed one position earlier than the wild type, as was the case for *bp-10* (Figures 1B, 1K, and 1M). These results suggest that *BP/KNAT1* prevents premature floral organ abscission.

### *BP/KNAT1* Regulates Floral Organ AZ Size and Organ Separation

To elucidate the role of *BP/KNAT1* further, scanning electron microscopy was performed. Petal abscission was carefully observed for the Col wild type and *bp-3* by either forceful removal of the petal or natural shedding at different stages of development (Figures 3A to 3C). Loss of *BP/KNAT1* in *bp-3* mutants affected the petal AZ fracture plane. In contrast with the wild type, which portrayed broken cells at positions 2 and 4, *bp-3* had broken cells at position 2 but a smooth fracture plane by position 4, first observed for the wild type at position 6 (Figure 3A). Initial rounding of AZ cells was observed as early as position 5 for *bp*-3 (as shown for position 6 in Figure 3A), comparable to position 7 in the wild type (Figure 3A). The *bp-3* mutant possessed fully rounded cells by position 7, similar to those seen in the wild type at position 8 (Figure 3A). The morphology of petal AZ cells was similar between *bp-3* and the wild type at position 12 (Figure 3A).

When comparing scanning electron micrographs of the whole abscission region, it was apparent that at the time of organ separation for *bp-3* (position 7), the discrete AZs found at the base of the receptacle in the wild type were less defined in the *bp-3* mutant. The filament AZ was larger than that of the wild type and extended closer to the valves of the silique than in the wild type, while the petal and sepal AZs were closer together and extended into the pedicel (Figure 3B). After organ separation (position 8 and 12), the AZ cell expansion was more pronounced, making it difficult to discriminate the petal and sepal AZs from

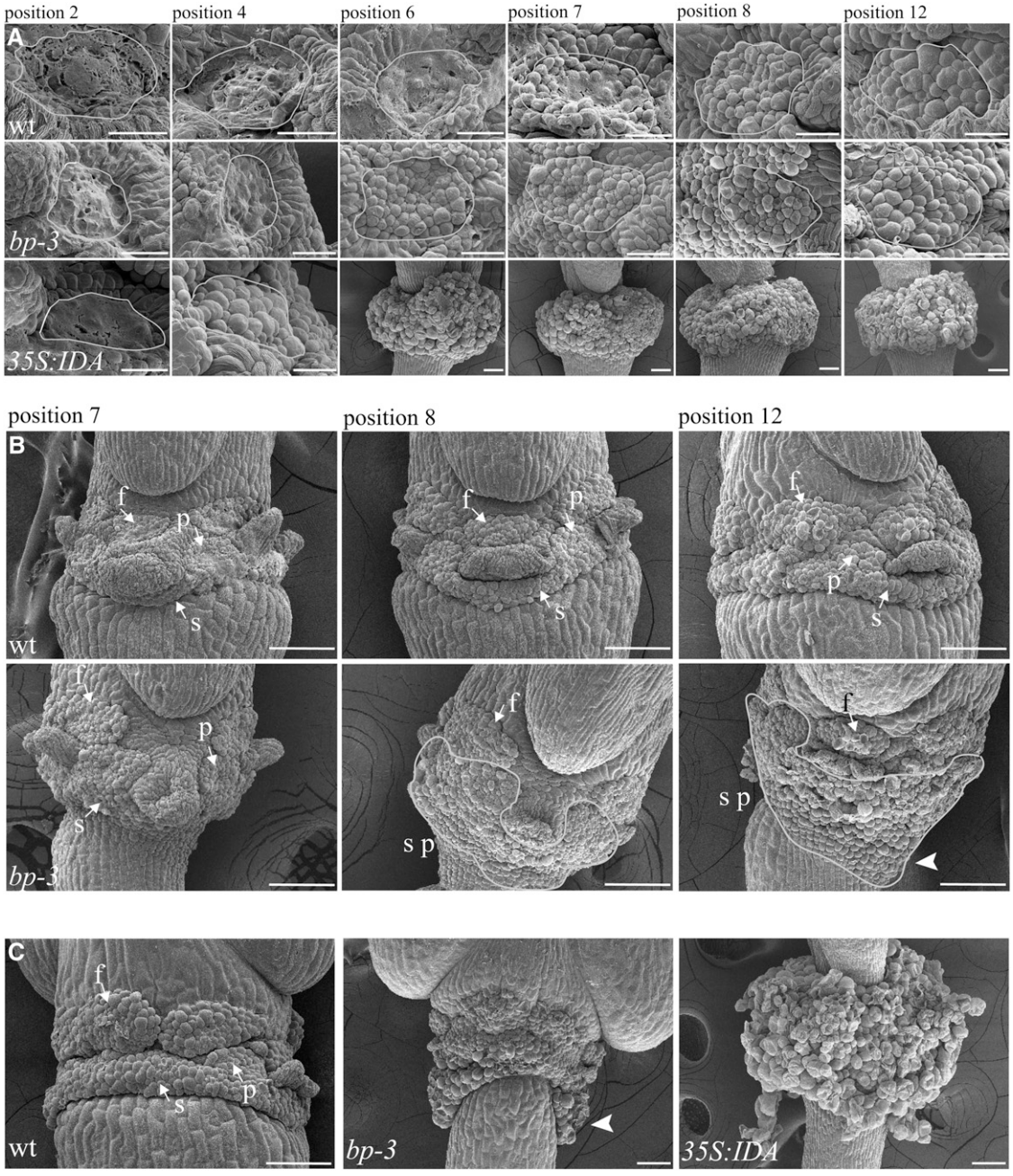


**Figure 3.** Floral AZ Scanning Electron Micrographs of *bp-3* and *35S:IDA*

**(A)** Fracture planes of petal AZ (delineated in gray) of the wild type (wt), *bp-3*, and *35S:IDA* at given floral positions. From position 6 onward, it is not possible to distinguish the different AZs for *35S:IDA* plants, and consequently the whole AZ region is shown for all positions older than position 6.
**(B)** Entire AZ region of the wild type and *bp-3* at given positions. Note that from position 8 onward in *bp-3*, it is not possible to distinguish the petal and sepal AZs from each other and the AZ region expands into the pedicel. The extended AZ region is delineated in gray.
**(C)** Entire AZ region of mature siliques. For *bp-3* and *35S:IDA*, it is not possible to indicate the different AZs.
f, filament AZ; p, petal AZ; s, sepal AZ. *bp-3* displays a larger sepal AZ region on the abaxial side of the pedicel (arrowhead in **[B]** and **[C]**). Bars = 30 μm for petal AZ fracture planes and 100 μm for the entire AZ region.

one another (Figure 3B). Interestingly, the normal symmetry seen in wild-type AZs was lost in *bp-3* mutants, and the sepal AZs on the abaxial side of the pedicel extended over a larger area (arrowhead in Figures 3B and 3C).

The resemblance between *bp-3* and flowers overexpressing IDA, such as the enlargement of the AZ region and the early cell wall loosening (Stenvik et al., 2006; Cho et al., 2008; Leslie et al., 2010), led us to ask the question whether the structural changes in AZ cells occurring during the abscission process would follow a similar progression. Compared with the broken cells observed in *bp-3*, *35S*:*IDA* had a flattened fracture cavity at position 2 and plants abscised their floral organs by position 4 where fully rounded AZ cells could be observed (Figure 3A). By comparing the petal AZ cell density of *bp-3* and *35S*:*IDA* to the wild type (Table 1), we found that both have increased cell size compared with the wild type at the positions where they shed their floral organs. These results, combined with the reduced pBS levels, suggest that cell elongation is important in regulating floral organ abscission and that *BP*/*KNAT1* plays a role in the proper timing of organ shedding by restricting cell expansion. In addition, we compared the height and width of petal AZs of *bp-3* and *35S*:*IDA* to those of wild-type plants at positions where the cell density between mutants and the wild type were approximately the same (Table 1). For both mutant and transgenic plants, there was a significant increase in size, indicating that the enlarged AZs observed (Figure 3C) are in part also due to an increase in AZ cell number.

A closer look at the AZ region revealed that *bp-3* and *bp-10* manifested a white substance surrounding the AZ region (Figures 1K and 1M). In *35S*:*IDA* plants, rounded AZ cells are gradually covered by a white substance consisting of high amounts of AG (Stenvik et al., 2006). When wild-type AZs are treated with the synthetic chemical reagent β-D-glucosyl Yariv (β-GlcY) (Yariv et al., 1962, 1967), which stains AG proteins (AGPs) red, staining is apparent in AZ cells at position 10, corresponding to the stage of organ separation. It has therefore been suggested that AGP secretion is a normal part of the abscission process (Stenvik et al., 2006). To assess the commonalities between *35S*:*IDA* and *bp-3* further, mature siliques of *bp-3* and *bp-10* were treated with β-GlcY and compared with *35S*:*IDA* (Figures 2C to 2E). The α-D-glucosyl Yariv does not bind AGPs and was used as a control (Figures 2F to 2H). This confirmed that the white substance covering the AZ region of *bp-3* and *bp-10* consisted in part of AGPs. Interestingly, a white substance was also observed at the base of *bp-3* mutant pedicels, as previously reported for activated vestigial AZs in *35S*:*IDA* plants (Stenvik et al., 2006). The similarity between *bp-3* and *35S*:*IDA* together with the rescue of organ separation in *bp ida-1*, *bp-3 ida-1*, and *bp-3 ida-2* indicate that *BP*/*KNAT1* and *IDA* act closely together to regulate floral organ abscission.

**Table 1.** Petal AZ Cell Density and Cell Number

| Cell Density in an Area of 1600 $\mu m^2$ | | | | |
|---|---|---|---|---|
| Genotype | p4 | p7 | p8 | p12 |
| Wild type | ND | 40 ± 1.83 | 30 ± 1.26 | 19 ± 0.89 |
| *bp-3* | ND | 30 ± 1.06* | 26 ± 1.11* | 19 ± 1.64 |
| *35S*:*IDA* | 29 ± 2.22 | 10 ± 1.21*[a] | 9 ± 0.63*[a] | 6 ± 1.29*[a] |
| Petal AZ cell number | | | | |
| Petal AZ | Wild type p8[b] | *35S*:*IDA* p4[b] | Wild type p12 | *bp-3* p12 |
| Height | 54.6 ± 4.55 | 60.7 ± 4.01* | 59.9 ± 3.43 | 78.2 ± 4.04* |
| Width | 87.8 ± 4.86 | 99.3 ± 9.49* | 98.9 ± 8.42 | 110.4 ± 6.59* |

p, positions; ND, not determined. Asterisks indicate significant differences ($P < 0.002$ for cell density and $P < 0.001$ for cell number) based on Student's *t* test; *n* (flowers) ≥ 4.

[a]At these stages, it is not possible to distinguish petal AZ for *35S*:*IDA*, and an area of 1600 $\mu m^2$ was measured within the AZ region.

[b]Positions where the wild type and *35S*:*IDA* have the same cell density.

## *BP*/*KNAT1* Is an Integral Component of the IDA-HAE/HSL2 Signaling Pathway

As IDA has been suggested to be the ligand of HAE and HSL2 (Cho et al., 2008; Stenvik et al., 2008) we used genetics to position *BP*/*KNAT1* relative to these genes. We created the triple mutant *bp-3 hae hsl2*, which showed an almost complete rescue of the floral abscission defect of *hae hsl2* (Figures 4A and 4B) with only some stamens attached on few siliques (Figure 4D). *ida-1 hae hsl2* plants are phenotypically identical to *hae hsl2* and are completely deficient in abscission. However, quadruple mutants of *bp ida-1 hae hsl2* (Figure 4C) had a similar but weaker rescue phenotype to that of *bp-3 hae hsl2* plants, with a larger proportion of the siliques having unabscised stamens (Figure 4E). The weaker rescue phenotype of *bp ida-1 hae hsl2* compared with *bp-3 hae hsl2* can be explained if we assume that the *bp-10* mutant, obtained from the backcross of *bp ida-1* to C24, retains some inhibitory activity lost in the null mutant *bp-3*. There could additionally be an effect of combining ecotypes. The observed phenotypes were further quantified by pBS measurements (Figure 4H), and the mature AZs of both *bp-3 hae hsl2* and *bp ida-1 hae hsl2* were covered with a white substance (Figures 4F and 4G).

These results suggest that BP/KNAT1 could be a downstream component of the IDA-HAE/HSL2 signaling pathway acting to inhibit premature organ separation, possibly by regulating genes involved in controlling cell expansion and cell division. We therefore analyzed the expression pattern of $BP/KNAT1_{pro}$:*GUS* in the AZs of *ida-2* and *hae hsl2* (see Supplemental Figures 4A and 4B online) to investigate whether *IDA*, *HAE*, and *HSL2* were regulating *BP*/*KNAT1* at the transcriptional level. No difference in the spatial or temporal distribution of *BP*/*KNAT1* could be observed in the mutant background compared with the wild type (see Supplemental Figure 4C online), and the relative expression levels of *BP*/*KNAT1* in *ida* and *hae hsl2* AZ tissue were unaltered (see Supplemental Figure 4D online). This indicates that *BP*/*KNAT1* could be regulated at the protein, rather than transcriptional, level by the IDA signaling pathway.

## The Inactivation of *KNAT2* and *KNAT6* Rescues the *bp-3* Floral Abscission Phenotype

*BP*/*KNAT1* is known to restrict the expression of *KNAT2* and *KNAT6* to promote correct inflorescence growth (Ragni et al., 2008). The inactivation of *KNAT6*, but not *KNAT2*, partially rescues the pedicel orientation phenotype of *bp*; however, a complete rescue of the downward-pointing siliques is seen in *bp*

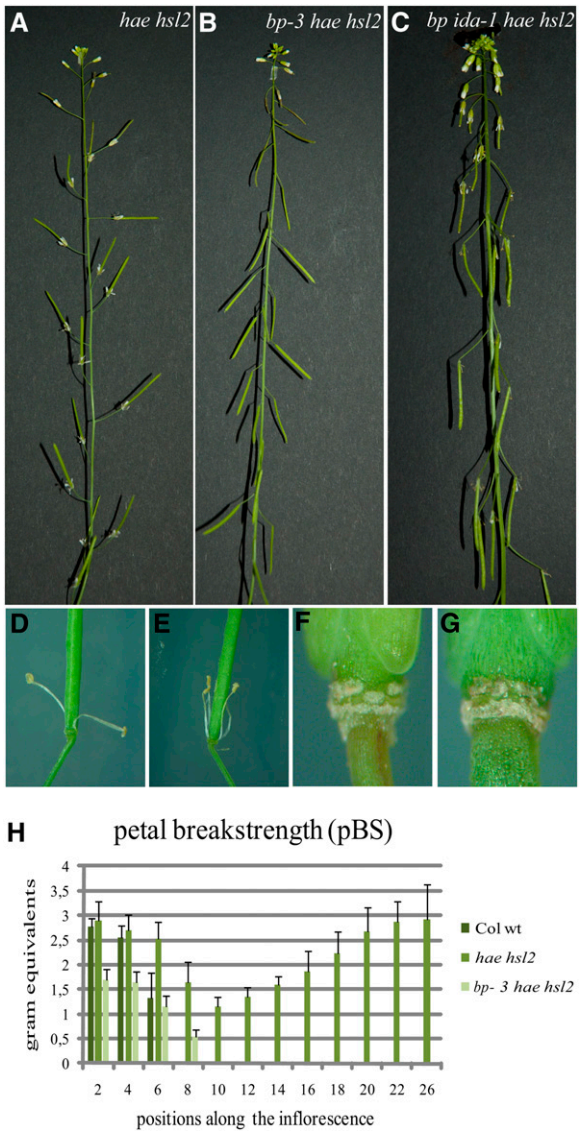


**Figure 4.** Genetic Interaction of *BP/KNAT1*, *HAE*, and *HSL2*.

**(A)** *hae hsl2* mutants with deficiency in floral abscission
**(B)** to **(G)** *bp* mutants rescue the abscission defect of *hae hsl2*. *bp-3 hae hsl2* main inflorescence **(B)**, silique at position 12 **(D)**, and AZ from mature silique **(F)**; *bp ida-1 hae hsl2* main inflorescence **(C)**, silique at position 12 **(E)**, and AZ from mature silique **(G)**.
**(H)** pBS of *bp-3 hae hsl2* compared with *hae hsl2* and Col wild type (wt). ($n$ = 15, bars = SD).
[See online article for color version of this figure.]

*knat2 knat6* triple mutants (Ragni et al., 2008). Therefore, we assayed the abscission phenotype of *bp-3* in single and double mutants of *knat2* and *knat6*. As expected, the downward orientations of siliques in *bp-3* was only partially rescued in *bp-3 knat6* and fully rescued in *bp-3 knat2 knat6* (Figures 5B to 5D). No difference was apparent in the AZ region of *bp-3 knat2* and *bp-3 knat6* compared with *bp-3* (Figures 5E and 5F). In both double mutants, the AZ was enlarged and covered with a white substance. However, pBS measurements suggest that there is a partial rescue of the early cell wall loosening of *bp-3* in *bp-3 knat6* (see Supplemental Figure 5A online), consistent for what is observed for the downward-pointing silique phenotype. Compared with each of the double mutants, *bp-3 knat2 knat6* triple mutant plants had delayed floral organ separation and the floral

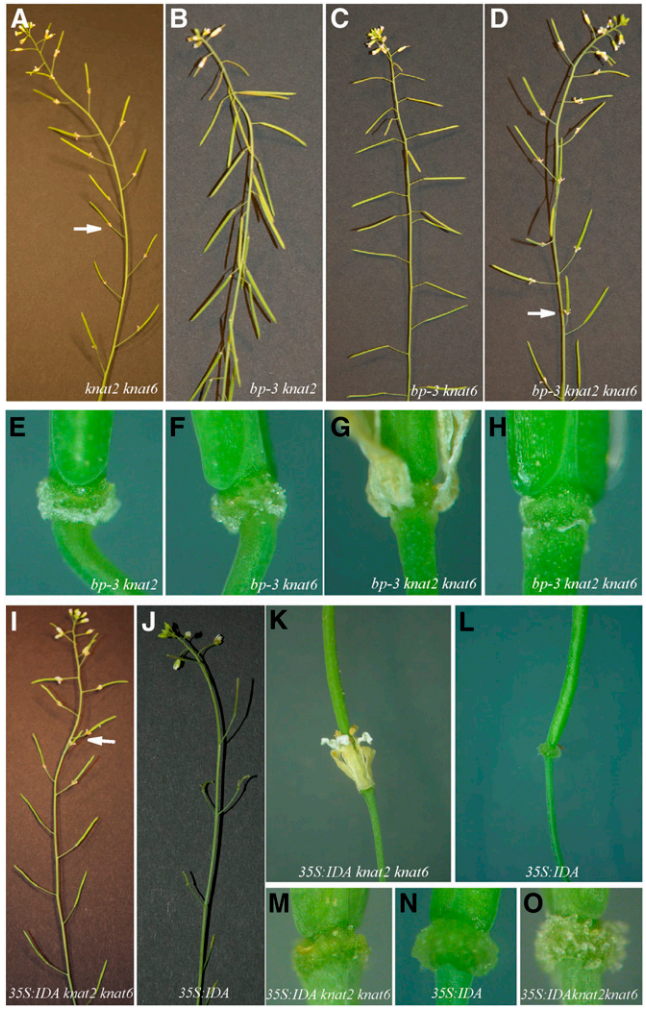


**Figure 5.** Phenotypes of *knat2* and *knat6* in *bp-3* and *35S:IDA*.

**(A)** Phenotype of *knat2 knat6* with organs attached at position 15 (arrow).
**(B)** to **(H)** Genetic interaction phenotypes of *knat2* and *knat6* with *bp-3*. *bp-3 knat2* (**[B]** and **[E]**), *bp-3 knat6* (**[C]** and **[F]**), and *bp-3 knat2 knat6* (**[D]**, **[G]**, and **[H]**). Inactivation of *knat6* but not *knat2* partially rescues the silique orientation phenotype of *bp-3* but not the enlarged AZ region. In *bp-3 knat2 knat6* triple mutants, siliques display wild-type orientation and a normal-sized AZ region with attached floral organs (arrow in **[D]**).
**(I)** and **(J)** Overexpression phenotypes of *35S:IDA* are not apparent in the *knat2 knat6* mutant background. Note floral organs attached in *35S:IDA knat2 knat6* (arrow).
**(K)** to **(N)** Siliques at position 7 have attached floral organs in *35S:IDA knat2 knat6* plants and normal-sized AZs (**[K]** and **[M]**) compared with *35S:IDA* (**[L]** and **[N]**).
**(O)** Mature *35S:IDA knat2 knat6* AZ with enlarged AZ region.
[See online article for color version of this figure.]

organs remained attached until at least position 15 (Figures 5D and 5G). Although no floral abscission defect has been reported for *knat2 knat6* double mutants (Belles-Boix et al., 2006; Ragni et al., 2008), we observed a delay in floral abscission (Figure 5A), which was accentuated with increased light intensity and which could not be distinguished from that in *bp-3 knat2 knat6* plants (Figure 5D). The forceful removal of floral organs from *bp-3 knat2 knat6* siliques revealed a normal AZ region with no apparent enlargement or secretion of white substance (Figure 5H). The same phenotypes were observed for *bp-3 ida-2 knat2 knat6* plants. Thus, the involvement of *BP/KNAT1* in regulating the correct timing of floral organ separation is likely dependent on its restrictive action on *KNAT2* and *KNAT6*.

### *knat2* and *knat6* Suppress the *35S:IDA* Phenotype

Since we observed that the premature time course of floral abscission in *bp-3* was rescued in *bp-3 knat2 knat6* triple mutants and that *bp-3* was capable of rescuing the abscission defect of *ida*, we examined the genetic interaction between the double mutant of *knat2 knat6* and a transgene overexpressing *IDA*. If the IDA signaling pathway negatively regulates *BP/KNAT1* and the restriction of *KNAT2* and *KNAT6* by *BP/KNAT1* is important for the correct timing of floral abscission, we hypothesized that the untimely organ loss in *35S:IDA* plants would be delayed in the *knat2 knat6* double mutant background.

In addition to the early floral abscission and enlarged AZ region, plants overexpressing *IDA* also have ectopic abscission of other organs, reduced stature, small siliques, and early senescence (Stenvik et al., 2006) (Figure 5J). Plants overexpressing *IDA* in the *knat2 knat6* double mutant background showed a wild-type phenotype at the whole-plant level (Figure 5I). The small siliques, which often senesce, on *35S:IDA* plants were absent in *35S:IDA knat2 knat6*. Moreover, the precocious floral abscission of *35S:IDA* plants, where all organs are shed by position 4 (Stenvik et al., 2006), was substantially delayed in *35S:IDA knat2 knat6* plants, and floral organs remained attached to the receptacle of the silique until at least position 15 (Figures 5K and 5L). The excessive AZ enlargement apparent in siliques of *35S:IDA* plants at position 7 (Figures 5L and 5N) was not observed in *35S:IDA knat2 knat6* (Figure 5M). However, as the siliques matured further, it was apparent that the AZ region of *35S:IDA knat2 knat6* plants became larger than that of the wild type (Figure 5O). The relative expression levels of *IDA* in *35S:IDA knat2 knat6* compared with the wild type verified that the observed phenotypes were not due to silencing of the transgene (see Supplemental Figure 5B online). Taken together, these results show that the phenotypes of *35S:IDA* plants are suppressed in the *knat2 knat6* mutant background and substantiates the hypothesis that the IDA signaling pathway is involved in the regulation of these genes through *BP/KNAT1*.

### *KNAT2* and *KNAT6* Are Transcriptionally Regulated by *IDA*, *HAE*, and *HSL2*

Since it has been shown that *BP/KNAT1* restricts the expression of *KNAT2* and *KNAT6* in pedicels (Ragni et al., 2008), we examined the expression patterns of *KNAT2* and *KNAT6* in *ida-1*, *hae hsl2*, and *bp* mutants during the different stages of floral organ abscission. We first examined *KNAT2* and *KNAT6* expression in the AZ of flowers along the whole length of the inflorescence using promoter:GUS transgenes ($KNAT2_{pro}$:*GUS* and $KNAT6_{pro}$:*GUS*) previously described by Ragni et al. (2008). In wild-type flowers, both *KNAT2* and *KNAT6* were expressed in the AZ region from early floral stages and up to the point of floral organ separation (Figures 6A and 6B). Both had an enhanced expression level at the stage of organ detachment, corresponding to position 10 for *KNAT2* in the C24 wild-type background (Figure 6A) and position 6-8 for *KNAT6* in the Wassilewskija (Ws) background (Figure 6B). *KNAT6* expression was restricted to the sepal, petal, and filament AZs in addition to the dehiscence zone of the silique, whereas *KNAT2* had a broader spatial distribution covering the entire AZ region (Figures 6A and 6B). By contrast, in the *ida-1* and *hae hsl2* AZs, the GUS expression of *KNAT2* and *KNAT6* was markedly reduced or totally absent, respectively (Figures 6C and 6D). The presence of $KNAT2_{pro}$:*GUS* expression at the base of *ida-1* and *hae hsl2* floral buds and $KNAT6_{pro}$:*GUS* expression in the vasculature of emerged lateral roots (Figures 6C and 6D), as previously reported for wild-type plants (Dean et al., 2004; Ragni et al., 2008), indicates that the expression of these genes in the mutant backgrounds is extenuated only in cells where *IDA*, *HAE*, and *HSL2* are normally expressed. Thus, during floral abscission, the expression of *KNAT2* and *KNAT6* in AZ tissue is dependent on the presence of *IDA*, *HAE*, and *HSL2*. Moreover, in the *bp* mutant background, an elevated level of *KNAT2* and *KNAT6* expression was observed in the AZ (Figures 6C and 6D), indicating that *BP/KNAT1* restricts the expression of *KNAT2* and *KNAT6* in AZ tissues in a similar way as in the pedicels.

### Misexpression of *KNAT2* and *KNAT6* Rescues the Floral Abscission Defect of *ida*

To extend further the genetic interaction study between *IDA*, *KNAT2*, and *KNAT6*, plants overexpressing *KNAT2* under an inducible cauliflower mosaic virus *35S* promoter in the Landsberg *erecta* (L*er*) wild-type background (Pautot et al., 2001) and a constitutively expressed *KNAT6* transgene in Col wild type (Figure 7A) were crossed into the *ida-1* mutant background. As expected if *KNAT2* and *KNAT6* are acting downstream in the IDA signaling pathway and are positive regulators of organ separation, misexpression of either gene in *ida-1* restored floral organ abscission (Figures 7B and 7C). Given that high levels of *KNAT2* expression leads to homeotic conversions of floral tissue (Pautot et al., 2001), we selected for plants with elevated expression levels of *KNAT2* that did not have severe developmental effects (see Supplemental Figure 6A online). pBS measurements for *35S:KNAT2 ida-1* showed a similar reduction compared with *ida-1* as that seen in the *bp-3 ida-1* double mutants (Figure 7D; see Supplemental Figure 2F online); however, it is possible that the contribution of the L*er* genome had an effect in the pBS. In addition, consistent with the pBS measurements showing a partial rescue of the early cell wall loosening of *bp-3* in *bp-3 knat6* double mutants (see Supplemental Figure 5A online), plants overexpressing *KNAT6* have lower pBS at all measurable positions compared with the Col wild type (see Supplemental Figure

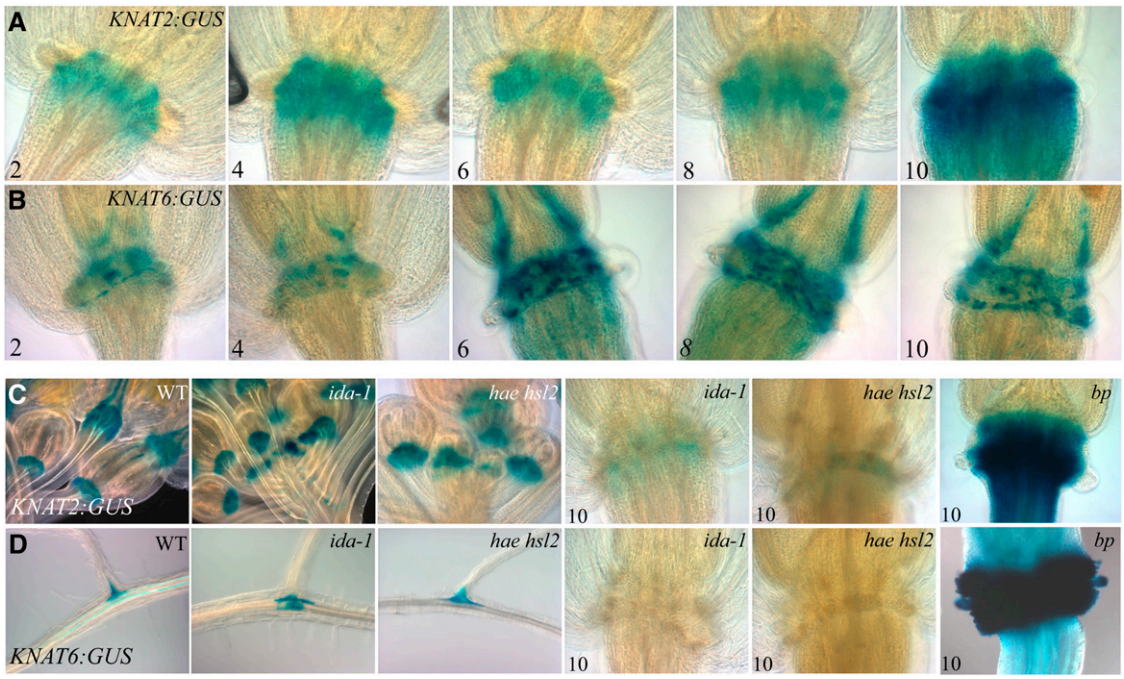


**Figure 6.** *KNAT2* and *KNAT6* Expression in *ida-1*, *hae hsl2*, and *bp* during Floral Abscission.

**(A)** *KNAT2* promoter-driven GUS expression during floral organ abscission in the C24 wild type.
**(B)** *KNAT6* promoter-driven GUS expression during floral organ abscission in the Ws wild type.
**(C)** *KNAT2* promoter-driven GUS expression in *ida-2*, *hae hsl2*, and *bp-3* AZs for flowers at position 10. GUS activity at the base of wild-type (wt) floral buds was unaltered in the *ida-2* and *hae hsl2* mutant backgrounds.
**(D)** *KNAT6* promoter-driven GUS expression in *ida-2*, *hae hsl2*, and *bp-9* (Ragni et al., 2008) AZs. GUS activity in the vasculature of emerging wild-type (wt) lateral roots was unaltered in the *ida-2* and *hae hsl2* mutant backgrounds.
Arabic numerals indicate floral positions along the inflorescence.

6B online). However, the AZ region is morphologically similar to that of the wild type (see Supplemental Figure 6C online). Taken together, these results indicate that *BP/KNAT1* acts as a negative regulator and *KNAT2* and *KNAT6* act as positive regulators of floral organ separation in the IDA signaling cascade.

## DISCUSSION

### The Role of *BP/KNAT1* in Floral Organ Abscission

In this article, we report on the characterization of a new mutant allele of *BP/KNAT1*, *bp-10*, and reveal a role for *BP/KNAT1* as a negative regulator of floral organ abscission. *BP/KNAT1* belongs to the super-class of TALE (three amino acid loop extension) HD proteins and is known to modulate various aspects of plant development, mainly by regulating cell growth and differentiation (Hamant and Pautot, 2010; Hay and Tsiantis, 2010).

We discovered a role for *BP/KNAT1* in abscission via a genetic screen for suppressors of the *ida-1* abscission deficiency. AZ cells differentiate early in floral development; however, loss of floral organs cannot be induced prior to anthesis, indicating that shortly after pollination the AZ cells become competent to respond to abscission signals (Patterson, 2001). Ethylene can expedite the abscission process (Van Doorn, 2002), suggesting that the timing of abscission can be modulated. *IDA* can induce cell separation from the time when AZ cells are able to respond to organ shedding signals, as seen by misexpression of *IDA*, which effectuates precocious floral abscission (Butenko et al., 2003; Stenvik et al., 2006). As described below, our results indicate that *BP/KNAT1* acts as a negative regulator of floral abscission by restricting AZ cell size and number and is likely suppressed by IDA signaling to allow for the progression of abscission.

In wild-type flowers, floral organ separation is preceded by a reduction in pBS that correlates with an initial rounding of AZ cells (Patterson, 2001). Loss of *BP/KNAT1*, as seen in the *bp-3* mutant, causes a substantial reduction in pBS at positions 2 and 4 (Figure 2B) and abscission of floral organs one position earlier than in wild-type inflorescences. In addition, compared with the wild type, the mutant has a significant ($P < 0.002$, Student's *t* test) enlargement of AZ cells at the time of organ separation, also seen for *35S:IDA* (Table 1). Although it is not completely clear what role cell expansion plays in the regulation of organ separation (Patterson, 2001), it is apparent that it correlates with the correct timing and the extent of the process. In *Arabidopsis*, the level of *EXP10* transcript, which encodes an expansin originally identified by its involvement in cell elongation (McQueen-Mason et al., 1992), regulates the degree of pedicel separation (Cho and Cosgrove, 2000). The loss of the LRR-RLK *EVR* shows increased floral AZ cell size and premature floral abscission in the *nev*

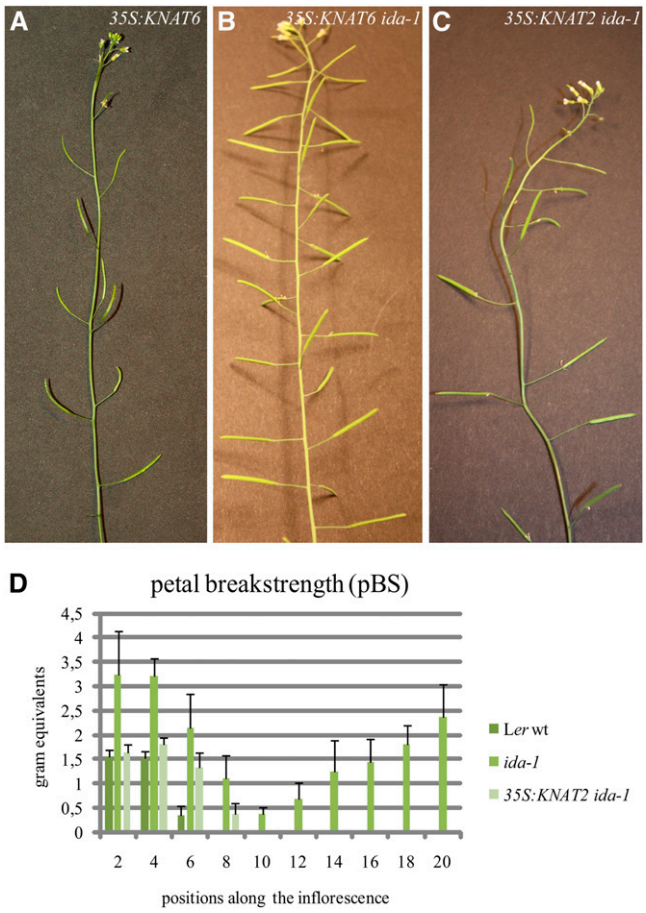


**Figure 7.** Overexpression of *KNAT2* and *KNAT6* in *ida-1*.

**(A)** *35S:KNAT6* (Col) inflorescence.
**(B)** and **(C)** *35S:KNAT6* (Col) and *35S:KNAT2* (L*er*) rescue the abscission defect of *ida-1*.
**(D)** pBS of *35S:KNAT2 ida-1* compared with *ida-1* and L*er* wild type (wt). ($n$ = 15, bars = SD).
[See online article for color version of this figure.]

background (Leslie et al., 2010). Interestingly, *EVR* is downregulated in *bp* mutants (Wang et al., 2006); however, unlike *bp ida-1* and *bp-3 ida-2* (Figure 1H; see Supplemental Figure 2 online), *evr ida-2* mutants have defective abscission (Leslie et al., 2010). Thus, *EVR* inhibits cell elongation and abscission independently of *IDA*, but *BP/KNAT1* may mediate crosstalk between the IDA-HAE/HSL2 and the *EVR* pathways (Figure 8). In some plant species, cells in the separation layers undergo cell division prior to abscission (Sexton and Roberts, 1982; Van Doorn and Stead, 1997) and so the increased number of petal AZ cells seen in the *bp-3* mutant (Table 1) could also contribute to the early abscission observed, as is the case for mutants of *SERK1* in the *nev* background (Lewis et al., 2010). During the development of leaf primordia, *BP/KNAT1* is directly repressed by ASYMMETRIC LEAVES2 (AS2) and AS1 (Ori et al., 2000). It has recently been shown that direct activation of *AS2* transcription by BOP1 and BOP2 is necessary for *BP/KNAT1* repression (Jun et al., 2010). It is therefore tempting to speculate that a similar mechanism is in place in AZ cells and that BP/KNAT1 could be acting to restrict AZ size and number by maintaining a boundary in the AZ region. However, the two scenarios differ: ectopic expression of *BP/KNAT1* prolongs leaf cell division (Chuck et al., 1996), whereas an increase in the number of AZ cells is observed when *BP/KNAT1* is mutated.

In the pedicel of *bp* loss-of-function mutants, growth is severely affected due to reduced cell division and less differentiation and elongation of cortical and epidermal cells on the abaxial side than on the adaxial side (Douglas et al., 2002; Venglat et al., 2002). Contrary to this, loss of *BP/KNAT1* in AZ cells

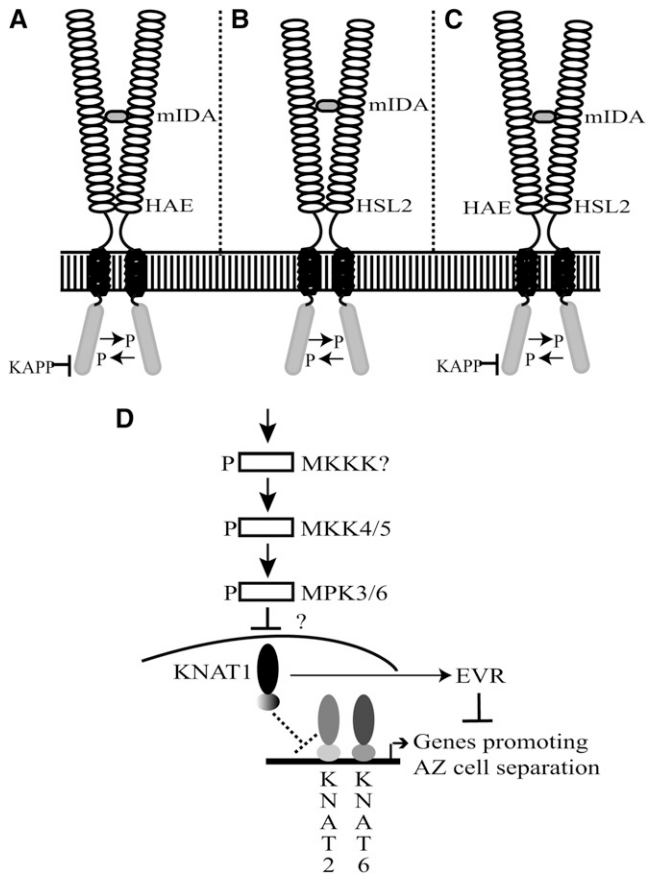


**Figure 8.** Models of IDA Signaling.

**(A)** to **(C)** IDA can be imagined to bind the extracellular LRRs of a HAE homodimer **(A)**, a HSL2 homodimer **(B)**, or a HAE-HSL2 heterodimer **(C)** and to cause autophosphorylation (P) of the kinase receptor domains. The protein phosphatase KAPP dephosphorylates HAE and returns the receptor to an off state (Stone et al., 1994).
**(D)** The signal from IDA-HAE/HSL2 is suggested to be transduced via a MAPK cascade that includes MKK4, MKK5, MPK3, and MPK6. Genetic evidence suggests that BP/KNAT1 acts as a negative downstream component of this signaling pathway by restricting cell wall degradation and consequently cell separation and the expression of *KNAT2* and *KNAT6*. Upon activation of the IDA signaling pathway, the BP/KNAT1 restriction of *KNAT2* and *KNAT6* is elevated, and these transcription factors can act as positive regulators of floral organ separation. In addition, BP/KNAT1 is a positive regulator of *EVR*, which influences cell elongation by a separate parallel pathway (Leslie et al., 2010).

enhances cell expansion and leads to an increased number of AZ cells (Table 1). It has been shown that *BP/KNAT1* transcripts are found in both the adaxial and the abaxial cortical cells of the pedicel tissue, suggesting that the transport of the *BP/KNAT1* transcript or protein may be involved in regulating the localized cell differentiation in the abaxial epidermal cells. This suggests that BP/KNAT1 acts differentially in different parts of the plant (Venglat et al., 2002; Kim et al., 2005; Rim et al., 2009) and that the phenotypic differences in *bp* mutant pedicels and AZ cells might be caused by perturbation of BP/KNAT1 interaction with other proteins in the AZ, such as BEL1-like (BELL) proteins (Bellaoui et al., 2001). Whereas the defect in pedicel cell differentiation in *bp* mutants has been attributed in part to the misregulation of genes involved in lignin biosynthesis (Mele et al., 2003), it is possible that the cellular defects observed in *bp-3* and *bp-10* during abscission affect the transcription of cell wall remodeling enzymes or genes that act to regulate cell wall remodeling enzymes. Since polygalacturonases have been shown to play an important role in cell separation during abscission, it would be interesting to monitor the expression levels of the two polygalacturonase-encoding genes *ARABIDOPSIS DEHISCENCE ZONE POLYGALACTURONASE2* and *QUARTET2* in *bp* mutants, as mutations in these genes delay floral abscission (González-Carranza et al., 2007; Ogawa et al., 2009). Since the functions of half of the TALE protein members remain unknown (Hamant and Pautot, 2010), it will be interesting to investigate if any have an abscission defect similar to that of *bp-3*.

### The Role of *KNAT2* and *KNAT6* in Floral Organ Abscission

The inflorescence phenotypic features of the *bp* mutant correlate with the misexpression of both *KNAT2* and *KNAT6*. Mutations in *KNAT6* can partially rescue the defects of *bp*, and normal pedicel development is observed in *bp knat2 knat6* mutants (Ragni et al., 2008). It has been proposed that BP/KNAT1 could directly regulate *KNAT2* and *KNAT6* expression, as motifs nearly identical to the *BP/KNAT1* binding site were found in *KNAT2* and *KNAT6* (Ragni et al., 2008); indeed, the expression levels of these genes is enhanced in floral AZs of *bp* mutants (Figures 6C and 6D). The triple mutant *bp-3 knat2 knat6* and the quadruple mutant *bp-3 ida-2 knat2 knat6* develop normal-sized AZs (Figures 5D and 5H) and are delayed in floral abscission (Figure 5G). This shows that *KNAT2* and *6* have antagonistic effects to those of *BP/KNAT1* during floral abscission and suggests that *KNAT2* and *6* are positive regulators of cell separation during floral abscission. It is tempting to speculate that *KNAT2* and/or *KNAT6* directly regulate AZ cell size. In part, this appears to be correct, in that plants overexpressing *IDA* in the *knat2 knat6* mutant background had smaller AZs compared with *35S:IDA* plants (Figures 5M and 5N) and were substantially delayed in abscission compared with *35S:IDA* (Figures 5K and 5L) and the wild type. However, in mature siliques of *35S:IDA knat2 knat6*, an increased AZ region was observed (Figure 5O) and *35S:KNAT6* plants show normal-sized AZs (see Supplemental Figure 6C online), indicating that additional factors must be in place to determine AZ cells size. This would also explain why the defect in floral abscission in *knat2 knat6* mutants is apparent only under certain growth conditions and why *35S:IDA* plants have stronger phenotypes than do *bp* mutants.

### Integration of the KNOX I Protein Family in the IDA Signaling Pathway

The isolation and characterization of *bp-10* in addition to the genetic and physiological analysis of *bp-3* allow us to expand the current model for IDA signaling. Our screen was designed to identify components of IDA signaling as revertants of the *ida-1* mutant abscission phenotype. As could be expected for negative downstream intermediates in this signaling pathway, *bp-3* mutations had features in common to *35S:IDA* plants: precocious cell wall loosening and cell elongation, increased AZ size, early abscission, and secretion of AGP. Moreover, both *bp-3* and *bp-10* could rescue the abscission defect of *hae hsl2* (Figures 4B and 4C). However, when comparing pBS between *bp-3* and Col wild type or between *bp-10* and C24 wild type, it was apparent that cell wall loosening was more accentuated in *bp-3* than in *bp-10* (Figure 2B). Moreover, the extent of rescue seen for *bp ida-1* and *bp ida-1 hae hsl2* was less than that observed for crosses with *bp*-3. This could be due to the molecular nature of *bp-10* compared with *bp-3*. The MEINOX domain, which for KNOX proteins is divided into two subdomains (KNOX1 and KNOX2) (Bürglin, 1997), is necessary for dimer formation with BELL proteins (Hay and Tsiantis, 2010) like PENNYWISE, which interacts with BP/KNAT1 and is thought to participate in repression of *KNAT2* and *KNAT6* (Smith and Hake, 2003; Ragni et al., 2008; Hay and Tsiantis, 2010). In *bp-10*, it is possible that a truncated protein with the KNOX1 domain, which has been shown to function as a repressor of transcription (Nagasaki et al., 2001), could be present. If so, and the truncated protein in part restricts *KNAT2* and *KNAT6*, this could explain that the *bp-10* allele is weaker than *bp-3*, which is a deletion mutant.

The findings that expression of *KNAT2* and *KNAT6* in AZ cells of *ida* and *hae hsl2* mutants was notably reduced and absent, respectively (Figures 6C and 6D), in addition to the complete rescue of the enlarged AZ region of *bp-3* by the *knat2 knat6* mutant, the reduction of *35S:IDA* phenotypes in *knat2 knat6*, and the rescue of *ida-1* by overexpression of *KNAT2* and *6* allow us to propose the following signaling pathway (Figure 8): A posttranslationally modified IDA protein (Stenvik et al., 2008) binds the LRR of either a homo or heterodimer including HAE and/or HSL2 and induces a MAPK signaling cascade that acts to regulate BP/KNAT1. Since the transcriptional levels of *BP/KNAT1* was unaltered in *ida* and *hae hsl2* (see Supplemental Figure 4 online), the regulation is likely to be at the protein level and could involve the interaction of BP/KNAT1 with another HD protein. BP/KNAT1 can then have a dual role both in regulating the expression of *EVR* and in restricting the expression of *KNAT2* and *KNAT6*, which in turn will positively regulate the transcription of genes involved in cell separation.

Future experiments investigating the cellular and subcellular localization of BP/KNAT1 during wild-type abscission compared with *ida* will likely give us information as to how the IDA signaling pathway is regulating the action of BP/KNAT1. Interestingly in the postabscission stages, the sepal AZ of *bp-3* mutants was not symmetrical and was larger on the abaxial side of the pedicel, indicating that at least in sepal AZ cells BP/KNAT1 could act differentially, similarly to what is seen for pedicel development (Venglat et al., 2002). This opens the possibility that IDA could

induce posttranslational modifications on BP/KNAT1 to regulate its trafficking in AZ cells.

## METHODS

### Growth Conditions

*Arabidopsis thaliana* plants were grown on soil in growth chambers at 22°C under long days (16 h day/8 h dark) at a light intensity of 100 $\mu E \cdot m^{-2} \cdot s^{-1}$. The floral abscission defect of the *knat2 knat6* double mutant was monitored at light intensities of 100 $\mu E \cdot m^{-2} \cdot s^{-1}$ and 250 $\mu E \cdot m^{-2} \cdot s^{-1}$.

### Ethyl Methanesulfonate Mutagenesis and Suppressor Mutant Screen

Approximately 50,000 *ida-1* (C24) seeds were treated with 0.3% ethyl methansulfonate (Sigma-Aldrich) for 16 h at room temperature in the dark. Seeds were then washed twenty times with deionized water, resuspended in 0.01% agar, and transferred to soil. Stratification was done for 1 week at 4°C, and plants were subsequently grown under standard conditions. M1 plants were harvested in pools of 10 plants. The frequency of chlorophyll mutants was 2%, determined by screening 1200 M2 plants.

The mutation points of line 49, line 595, and line 221 were determined by sequencing of their *BP/KNAT1* gene region amplified with *KNAT1 F* and *KNAT1 R* primers.

### Primers

Sequences of all primers used can be found in Supplemental Table 1 online.

### Plant Material and Genetic Crosses

Mutant alleles and transgenic plants described previously include *ida-1* (C24) (Butenko et al., 2003), *ida-2* (Col) (Cho et al., 2008), *hae hsl2* (Col) (Cho et al., 2008; Stenvik et al., 2008), *bop1 bop2* (Col) (Hepworth et al., 2005; Norberg et al., 2005), *35S:IDA* (C24) (Stenvik et al., 2006), *knat2 knat6*, $KNAT2_{pro}$:*GUS* (C24), $KNAT6_{pro}$:*GUS* (Ws and Col), $KNAT6_{pro}$:*GUS bp-9* (Ragni et al., 2008), and *35S:KNAT2* (L*er*) (Pautot et al., 2001). The transgenic Col line $BP/KNAT1_{pro}$:*GUS* (N6141) (Ori et al., 2000) was obtained from the Nottingham Arabidopsis Stock Centre, and *bp-3* (Col) (Rim et al., 2009) was kindly provided by Jae-Yean Kim. The *bp- 10* allele was generated through the backcross between *bp ida-1* and C24 wild-type plants with subsequent genotyping with *ida-1* genotyping primers and *GUS64L*. Homozygous $BP/KNAT1_{pro}$:*GUS*, $KNAT2_{pro}$:*GUS*, and $KNAT6_{pro}$:*GUS* lines were crossed to *ida-1* or *ida-2* and *hae hsl2*. F2 plants with deficiency in abscission were selected for GUS staining. Homozygous $KNAT2_{pro}$:*GUS* was crossed to *bp-3* and F2 plants with downward-pointing siliques were selected for GUS staining. *bp-3* was crossed to *ida-1*, *ida-2*, *hae hsl2*, *bop1 bop2*, and *knat2 knat6*, respectively. Double and triple mutants were verified by PCR with the corresponding genotyping primers and *Lbb1* (or *GUS64L* for *ida-1*). *bp ida-1* was crossed to *hae hsl2* and *bop1 bop2*. Quadruple mutants were verified by PCR with the corresponding genotyping primers, *Lbb1*, and cleaved-amplified polymorphic sequence marker (see Supplemental Table 1 online). *knat2 knat6* was crossed to *bp-3*, *bp-3 ida-2*, and *35S:IDA*, respectively. *bp-3 knat2*, *bp-3 knat6*, *bp-3 knat2 knat6*, *bp-3 ida-2 knat2*, *bp-3 ida-2 knat6*, *bp-3 ida-2 knat2 knat6*, and *35S:IDA knat2 knat6* were selected by PCR in the F2 or F3 population with corresponding genotyping primers. *35S:KNAT2* and *35S:KNAT6* were crossed to *ida-1*, and the transgenes in *ida-1* were selected by phenotype, PCR, and fluorescent selection for *35S:KNAT6* (described by Bensmihen et al., 2004).

### Generation of Transgenic Plants

For the complementation test, the genomic *BP/KNAT1* region was amplified by PCR from BAC F9M13 with the primers *attB1KNAT1* and *attB2KNAT1* with additional gateway *attB* sequences at the 5′ ends and introduced into the pDONR/Zeo gateway vector (Invitrogen). The 3.2-kb fragment was thereafter recombined through the entry clone into the pH7WG2 destination vector (Karimi et al., 2002). The construct was transferred to the *Agrobacterium tumefaciens* strain C58C1 pGV2260, and *bp ida-2* plants and C24 wild-type plants were transformed using the *A. tumefaciens*–mediated floral dip method (Clough and Bent, 1998). Transgenic plants were selected for resistance on medium (Murashige and Skoog, 1962) with 50 $\mu$g/mL hygromycin. Thirty-six out of 54 transformants showed the characteristic lobed leaf phenotype of *35S:KNAT1* plants.

The *KNAT6* cDNA was amplified using primers specific to *KNAT6* and cloned into the pCR II TOPO blunt vector (Invitrogen). Subsequently, the primers *attB1KNAT6* and *attB2KNAT6* were used to amplify *KNAT6* and recombine the gene into pDONR201 (Invitrogen). *KNAT6* was thereafter introduced by recombination into the binary destination alligator 2 vector by Gateway recombination. This vector allows for the selection of transgenic *Arabidopsis* seeds via GFP expression driven by the At2S3 seed-specific promoter by Bensmihen et al. (2004). The new vector called alli2KNAT6, harboring the HA-KNAT6 fusion under the double enhanced cauliflower promoter, was introduced into *A. tumefaciens* strain C58, and C24 wild-type plants were transformed using the *A. tumefaciens*–mediated floral dip method (Clough and Bent, 1998).

### Histochemical GUS Assay and β-GlcY Staining

GUS staining, postfixation, and whole-mount clearing preparations of various plant tissues were performed as described (Grini et al., 2002) and inspected with a Zeiss Axioplan2 imaging microscope equipped with differential interference contrast optics and a cooled Axiocam camera imaging system.

β-GlcY (Biosupplies) was used to test for the presence of AGPs, whereas α-GlcY (Biosupplies) was used as a negative control. Plant tissues were treated as previously described (Stenvik et al., 2006).

### Quantitative Real-Time RT-PCR

Total RNA was extracted from rosette leaves and floral AZs (position 4 to 8) using the spectrum plant total RNA kit (Sigma-Aldrich) according to the manufacturer's recommendations. An optional on-column DNase digestion step was included. cDNA synthesis and real-time RT-PCR were performed as described previously (Grini et al., 2009). Gene amplification was performed using the primers denoted in Supplemental Table 1 online. For all samples, cDNAs were normalized using *RCAR1* (At1g01360) and primers *CAB F* and *CAB R*.

### Breakstrength Measurement

pBS was quantified as the force in gram equivalents required for removal of a petal from a flower (Butenko et al., 2003) and was performed as described by Stenvik et al. (2008). Breakstrength was measured for 15 plants and a minimum of 20 measurements at each position.

### Scanning Electron Microscopy

Plant tissues for electron microscopy were fixed and dehydrated as described previously (Butenko et al., 2003) and critical point dried using a Bal-Tec CPD030 critical point dryer. Specimens were mounted on carbon tape and sputter coated with gold palladium using a Cressington Coating System 308R. Samples were viewed at a 5K accelerating voltage on a

S-4800 field emission scanning electron microscope (Hitachi). AZ measurements were performed using NIH Image software. To determine the cell density of petal AZs, cells that fell completely or partially within a 1600 $\mu m^2$ area in a petal AZ were counted, and a minimum of four flowers were used; for *35S:IDA* flowers older than position 4, it was not possible to distinguish individual petal AZ and an area of 1600 $\mu m^2$ in the AZ region was used. To determine the cell number of petal AZs, the height and width of petal AZs were measured at positions with similar cell density.

### Accession Numbers

Sequence data from this article can be found in the GenBank/EMBL data libraries under accession numbers At1g68765 (*IDA*), At4g28490 (*HAE*), At5g65710 (*HSL2*), At4g08150 (*BP*/*KNAT1*), At1g70510 (*KNAT2*), At1g23380 (*KNAT6*), At3g57130 (*BOP1*), and At2g41370 (*BOP2*).

### Supplemental Data

The following materials are available in the online version of this article.

**Supplemental Figure 1.** Phenotypes and Mutation Points of Revertant Lines.

**Supplemental Figure 2.** Genetic Interaction of *BP*/*KNAT1* and *IDA*.

**Supplemental Figure 3.** *BP*/*KNAT1* Expression and Genetic Interaction with *bop1 bop2*.

**Supplemental Figure 4.** *BP*/*KNAT1* Expression in *ida-2* and *hae hsl2*.

**Supplemental Figure 5.** Rescue of Precocious *bp-3* Cell Loosening by *knat2* and *knat6*.

**Supplemental Figure 6.** Contribution of *35S:KNAT2* and *35S:KNAT6* to Floral Abscission.

**Supplemental Table 1.** Primers.

## ACKNOWLEDGMENTS

We thank Jae-Yean Kim for the *bp-3* seeds, Solveig Hauge Engebretsen and Roy Falleth for technical assistance, the electron microscopy facility at the University of Oslo for assistance with scanning electron microscopy, and Reza Shirzadi for the *CAB F* and *CAB R* primers. The pDONR201-KNAT6 cDNA was cloned as part of the REGIA project by Enric Belle-Boix. This work was supported by Grants 175238/S10 (to C.-L.S., G.-E.S., A.K.V., R.B.A., and A.M.B.) and 178049 (to M.A.B., R.B.A., and A.M.B.) from the Research Council of Norway.

## AUTHOR CONTRIBUTIONS

C.-L.S. and M.A.B. designed the research. C.-L.S., G.-E.S., A.K.V., V.P., and M.A.B. performed the research. C.-L.S., R.B.A., and M.A.B. analyzed the data. R.B.A., V.P., M.P., and A.M.B. contributed reagents, materials, and analysis tools. M.A.B. wrote the article.

Received February 23, 2011; revised June 1, 2011; accepted June 19, 2011; published July 8, 2011.

## REFERENCES

**Aalen, R.B.** (2011). Flower and floral organ abscission: Control, gene expression and hormone interaction. In The Flowering Process and Its Control in Plants: Gene Expression and Hormone Interaction, M.W. Yaish, ed (Kerala, India: Research Signpost/Transworld Research Network), pp. 307–327.

**Alonso-Cantabrana, H., Ripoll, J.J., Ochando, I., Vera, A., Ferrándiz, C., and Martínez-Laborda, A.** (2007). Common regulatory networks in leaf and fruit patterning revealed by mutations in the *Arabidopsis ASYMMETRIC LEAVES1* gene. Development **134:** 2663–2671.

**Bellaoui, M., Pidkowich, M.S., Samach, A., Kushalappa, K., Kohalmi, S.E., Modrusan, Z., Crosby, W.L., and Haughn, G.W.** (2001). The *Arabidopsis* BELL1 and KNOX TALE homeodomain proteins interact through a domain conserved between plants and animals. Plant Cell **13:** 2455–2470.

**Belles-Boix, E., Hamant, O., Witiak, S.M., Morin, H., Traas, J., and Pautot, V.** (2006). *KNAT6*: An *Arabidopsis* homeobox gene involved in meristem activity and organ separation. Plant Cell **18:** 1900–1907.

**Bensmihen, S., To, A., Lambert, G., Kroj, T., Giraudat, J., and Parcy, F.** (2004). Analysis of an activated *ABI5* allele using a new selection method for transgenic *Arabidopsis* seeds. FEBS Lett. **561:** 127–131.

**Bleecker, A.B., and Patterson, S.E.** (1997). Last exit: Senescence, abscission, and meristem arrest in *Arabidopsis*. Plant Cell **9:** 1169–1179.

**Bürglin, T.R.** (1997). Analysis of TALE superclass homeobox genes (MEIS, PBC, KNOX, Iroquois, TGIF) reveals a novel domain conserved between plants and animals. Nucleic Acids Res. **25:** 4173–4180.

**Butenko, M.A., Patterson, S.E., Grini, P.E., Stenvik, G.-E., Amundsen, S.S., Mandal, A., and Aalen, R.B.** (2003). *Inflorescence deficient in abscission* controls floral organ abscission in *Arabidopsis* and identifies a novel family of putative ligands in plants. Plant Cell **15:** 2296–2307.

**Cho, H.-T., and Cosgrove, D.J.** (2000). Altered expression of expansin modulates leaf growth and pedicel abscission in *Arabidopsis thaliana*. Proc. Natl. Acad. Sci. USA **97:** 9783–9788.

**Cho, S.K., Larue, C.T., Chevalier, D., Wang, H., Jinn, T.L., Zhang, S., and Walker, J.C.** (2008). Regulation of floral organ abscission in *Arabidopsis thaliana*. Proc. Natl. Acad. Sci. USA **105:** 15629–15634.

**Chuck, G., Lincoln, C., and Hake, S.** (1996). KNAT1 induces lobed leaves with ectopic meristems when overexpressed in *Arabidopsis*. Plant Cell **8:** 1277–1289.

**Clough, S.J., and Bent, A.F.** (1998). Floral dip: A simplified method for *Agrobacterium*-mediated transformation of *Arabidopsis thaliana*. Plant J. **16:** 735–743.

**Dean, G., Casson, S., and Lindsey, K.** (2004). *KNAT6* gene of *Arabidopsis* is expressed in roots and is required for correct lateral root formation. Plant Mol. Biol. **54:** 71–84.

**Douglas, S.J., Chuck, G., Dengler, R.E., Pelecanda, L., and Riggs, C.D.** (2002). *KNAT1* and *ERECTA* regulate inflorescence architecture in *Arabidopsis*. Plant Cell **14:** 547–558.

**Fernandez, D.E., Heck, G.R., Perry, S.E., Patterson, S.E., Bleecker, A.B., and Fang, S.C.** (2000). The embryo MADS domain factor AGL15 acts postembryonically. Inhibition of perianth senescence and abscission via constitutive expression. Plant Cell **12:** 183–198.

**González-Carranza, Z.H., Elliott, K.A., and Roberts, J.A.** (2007). Expression of polygalacturonases and evidence to support their role during cell separation processes in *Arabidopsis thaliana*. J. Exp. Bot. **58:** 3719–3730.

**Grini, P.E., Jürgens, G., and Hülskamp, M.** (2002). Embryo and endosperm development is disrupted in the female gametophytic capulet mutants of *Arabidopsis*. Genetics **162:** 1911–1925.

**Grini, P.E., Thorstensen, T., Alm, V., Vizcay-Barrena, G., Windju, S.S., Jørstad, T.S., Wilson, Z.A., and Aalen, R.B.** (2009). The *ASH1 HOMOLOG 2* (*ASHH2*) histone H3 methyltransferase is required for ovule and anther development in *Arabidopsis*. PLoS ONE **4:** e7817.

**Hamant, O., and Pautot, V.** (2010). Plant development: A TALE story. C. R. Biol. **333:** 371–381.

**Hay, A., and Tsiantis, M.** (2010). KNOX genes: Versatile regulators of plant development and diversity. Development **137:** 3153–3165.

**Hepworth, S.R., Zhang, Y., McKim, S., Li, X., and Haughn, G.W.**

(2005). *BLADE-ON-PETIOLE*-dependent signaling controls leaf and floral patterning in *Arabidopsis*. Plant Cell **17:** 1434–1448.

**Jinn, T.-L., Stone, J.M., and Walker, J.C.** (2000). *HAESA*, an Arabidopsis leucine-rich repeat receptor kinase, controls floral organ abscission. Genes Dev. **14:** 108–117.

**Jun, J.H., Ha, C.M., and Fletcher, J.C.** (2010). BLADE-ON-PETIOLE1 coordinates organ determinacy and axial polarity in *Arabidopsis* by directly activating ASYMMETRIC LEAVES2. Plant Cell **22:** 62–76.

**Karimi, M., Inzé, D., and Depicker, A.** (2002). GATEWAY vectors for *Agrobacterium*-mediated plant transformation. Trends Plant Sci. **7:** 193–195.

**Kim, J.Y., Rim, Y., Wang, J., and Jackson, D.** (2005). A novel cell-to-cell trafficking assay indicates that the KNOX homeodomain is necessary and sufficient for intercellular protein and mRNA trafficking. Genes Dev. **19:** 788–793.

**Lease, K.A., Cho, S.K., and Walker, J.C.** (2006). A petal breakstrength meter for *Arabidopsis* abscission studies. Plant Methods **2:** 2.

**Leslie, M.E., Lewis, M.W., Youn, J.Y., Daniels, M.J., and Liljegren, S.J.** (2010). The EVERSHED receptor-like kinase modulates floral organ shedding in *Arabidopsis*. Development **137:** 467–476.

**Lewis, M.W., Leslie, M.E., Fulcher, E.H., Darnielle, L., Healy, P.N., Youn, J.Y., and Liljegren, S.J.** (2010). The SERK1 receptor-like kinase regulates organ separation in *Arabidopsis* flowers. Plant J. **62:** 817–828.

**Lewis, M.W., Leslie, M.E., and Liljegren, S.J.** (2006). Plant separation: 50 ways to leave your mother. Curr. Opin. Plant Biol. **9:** 59–65.

**Liljegren, S.J., Leslie, M.E., Darnielle, L., Lewis, M.W., Taylor, S.M., Luo, R., Geldner, N., Chory, J., Randazzo, P.A., Yanofsky, M.F., and Ecker, J.R.** (2009). Regulation of membrane trafficking and organ separation by the NEVERSHED ARF-GAP protein. Development **136:** 1909–1918.

**Lincoln, C., Long, J., Yamaguchi, J., Serikawa, K., and Hake, S.** (1994). A knotted1-like homeobox gene in *Arabidopsis* is expressed in the vegetative meristem and dramatically alters leaf morphology when overexpressed in transgenic plants. Plant Cell **6:** 1859–1876.

**McKim, S.M., Stenvik, G.-E., Butenko, M.A., Kristiansen, W., Cho, S.K., Hepworth, S.R., Aalen, R.B., and Haughn, G.W.** (2008). The *BLADE-ON-PETIOLE* genes are essential for abscission zone formation in *Arabidopsis*. Development **135:** 1537–1546.

**McQueen-Mason, S., Durachko, D.M., and Cosgrove, D.J.** (1992). Two endogenous proteins that induce cell wall extension in plants. Plant Cell **4:** 1425–1433.

**Mele, G., Ori, N., Sato, Y., and Hake, S.** (2003). The knotted1-like homeobox gene *BREVIPEDICELLUS* regulates cell differentiation by modulating metabolic pathways. Genes Dev. **17:** 2088–2093.

**Mukherjee, K., Brocchieri, L., and Bürglin, T.R.** (2009). A comprehensive classification and evolutionary analysis of plant homeobox genes. Mol. Biol. Evol. **26:** 2775–2794.

**Murashige, T., and Skoog, F.** (1962). A revised medium for rapid growth and bio assays with tobacco tissue cultures. Physiol. Plant. **15:** 473–497.

**Nagasaki, H., Sakamoto, T., Sato, Y., and Matsuoka, M.** (2001). Functional analysis of the conserved domains of a rice KNOX homeodomain protein, OSH15. Plant Cell **13:** 2085–2098.

**Norberg, M., Holmlund, M., and Nilsson, O.** (2005). The *BLADE ON PETIOLE* genes act redundantly to control the growth and development of lateral organs. Development **132:** 2203–2213.

**Ogawa, M., Kay, P., Wilson, S., and Swain, S.M.** (2009). ARABIDOPSIS DEHISCENCE ZONE POLYGALACTURONASE1 (ADPG1), ADPG2, and QUARTET2 are Polygalacturonases required for cell separation during reproductive development in *Arabidopsis*. Plant Cell **21:** 216–233.

**Ori, N., Eshed, Y., Chuck, G., Bowman, J.L., and Hake, S.** (2000). Mechanisms that control knox gene expression in the *Arabidopsis* shoot. Development **127:** 5523–5532.

**Patterson, S.E.** (2001). Cutting loose. Abscission and dehiscence in Arabidopsis. Plant Physiol. **126:** 494–500.

**Patterson, S.E., and Bleecker, A.B.** (2004). Ethylene-dependent and -independent processes associated with floral organ abscission in *Arabidopsis*. Plant Physiol. **134:** 194–203.

**Pautot, V., Dockx, J., Hamant, O., Kronenberger, J., Grandjean, O., Jublot, D., and Traas, J.** (2001). *KNAT2*: Evidence for a link between knotted-like genes and carpel development. Plant Cell **13:** 1719–1734.

**Ragni, L., Belles-Boix, E., Günl, M., and Pautot, V.** (2008). Interaction of *KNAT6* and *KNAT2* with *BREVIPEDICELLUS* and *PENNYWISE* in *Arabidopsis* inflorescences. Plant Cell **20:** 888–900.

**Rim, Y., Jung, J.-H., Chu, H., Cho, W.K., Kim, S.-W., Hong, J.C., Jackson, D., Datla, R., and Kim, J.-Y.** (2009). A non-cell-autonomous mechanism for the control of plant architecture and epidermal differentiation involves intercellular trafficking of BREVIPEDICELLUS protein. Plant Biol. **36:** 280–289.

**Roberts, J.A., Elliott, K.A., and Gonzalez-Carranza, Z.H.** (2002). Abscission, dehiscence, and other cell separation processes. Annu. Rev. Plant Biol. **53:** 131–158.

**Scofield, S., and Murray, J.A.H.** (2006). *KNOX* gene function in plant stem cell niches. Plant Mol. Biol. **60:** 929–946.

**Sexton, R., and Redshaw, A.J.** (1981). The role of cell expansion in the abcission of *Impatiens* leaves. Ann. Bot. (Lond.) **48:** 745–757.

**Sexton, R., and Roberts, J.A.** (1982). Cell biology of abscission. Annu. Rev. Plant Physiol. **33:** 133–162.

**Smith, H.M.S., and Hake, S.** (2003). The interaction of two homeobox genes, *BREVIPEDICELLUS* and *PENNYWISE*, regulates internode patterning in the *Arabidopsis* inflorescence. Plant Cell **15:** 1717–1727.

**Smyth, D.R., Bowman, J.L., and Meyerowitz, E.M.** (1990). Early flower development in *Arabidopsis*. Plant Cell **2:** 755–767.

**Stenvik, G.E., Butenko, M.A., Urbanowicz, B.R., Rose, J.K., and Aalen, R.B.** (2006). Overexpression of *INFLORESCENCE DEFICIENT IN ABSCISSION* activates cell separation in vestigial abscission zones in *Arabidopsis*. Plant Cell **18:** 1467–1476.

**Stenvik, G.-E., Tandstad, N.M., Guo, Y., Shi, C.-L., Kristiansen, W., Holmgren, A., Clark, S.E., Aalen, R.B., and Butenko, M.A.** (2008). The EPIP peptide of INFLORESCENCE DEFICIENT IN ABSCISSION is sufficient to induce abscission in *arabidopsis* through the receptor-like kinases HAESA and HAESA-LIKE2. Plant Cell **20:** 1805–1817.

**Stone, J.M., Collinge, M.A., Smith, R.D., Horn, M.A., and Walker, J.C.** (1994). Interaction of a protein phosphatase with an *Arabidopsis* serine-threonine receptor kinase. Science **266:** 793–795.

**Van Doorn, W.G.** (2002). Effect of ethylene on flower abscission: A survey. Ann. Bot. (Lond.) **89:** 689–693.

**Van Doorn, W.G., and Stead, A.D.** (1997). Abscission of flowers and floral parts. J. Exp. Bot. **48:** 821–837.

**Venglat, S.P., Dumonceaux, T., Rozwadowski, K., Parnell, L., Babic, V., Keller, W., Martienssen, R., Selvaraj, G., and Datla, R.** (2002). The homeobox gene *BREVIPEDICELLUS* is a key regulator of inflorescence architecture in *Arabidopsis*. Proc. Natl. Acad. Sci. USA **99:** 4730–4735.

**Wang, X.-Q., Xu, W.-H., Ma, L.-G., Fu, Z.-M., Deng, X.-W., Li, J.-Y., and Wang, Y.-H.** (2006). Requirement of *KNAT1/BP* for the development of abscission zones in *Arabidopsis thaliana*. J. Integr. Plant Biol. **48:** 15–26.

**Yariv, J., Rapport, M.M., and Graf, L.** (1962). The interaction of glycosides and saccharides with antibody to the corresponding phenylazo glycosides. Biochem. J. **85:** 383–388.

**Yariv, J., Lis, H., and Katchalski, E.** (1967). Precipitation of arabic acid and some seed polysaccharides by glycosylphenylazo dyes. Biochem. J. **105:** 1C–2C.